BUTTERWORTH HEINEMANN

Visualization of dynamic simulations of muscle thin filaments

Guangzhou Zou,* G. Anthony Gorry,* and George N. Phillips, Jr.†

**Department of Computer Science and †Department of Biochemistry and Cell Biology, W.M. Keck Center for Computational Biology, Rice University, Houston, Texas*

Following a novel computational formalism, the thin filament of muscle can be modeled by a computational machine containing a large number of finite automata that have one-to-one correspondence with the constituent protein molecules.[1] Computer graphics can be used to visualize the correspondence between the states of finite automata and the configurations of protein molecules according to the structural data. The dynamic simulation of the muscle filament that corresponds to the concurrent state transitions of finite automata can be represented as a sequence of video images. The kinetic and structural knowledge of individual protein molecules is, therefore, integrated into a coherent and functional system. This type of computation and visualization can also be useful for the investigation of molecular structure, function, and interaction in various complex biological systems.

Keywords: cellular automata, muscle regulation, structure of muscle thin filament, video imaging, isosurface, 3D animation

INTRODUCTION

A physical process can be abstracted as a computing process. Various phenomena in the world can be considered as some sort of ongoing computations in the sense that nature is continually computing the "next state" of the universe. We can use the term *information mechanics*[2] to refer to the computational aspect of a natural phenomenon.

First, let us compare the act of performing a computation with that of performing a biochemical or physiological experiment.

In a computation, we have a computational system **C**. We start **C** in specified initial conditions a, let **C** run for a certain time, and then look at its final conditions b. The process can be represented as

$$a \rightarrow \boxed{\mathbf{C}} \rightarrow b$$

Here, we have a complete knowledge about **C** and know exactly how conditions a are transformed into b.

In a biochemical or physiological experiment, we have a certain selected biological system **B,** the experimental setup. We provide initial conditions α, let **B** run for a certain time, and then look at its final condition β. The process can be represented as

$$\alpha \rightarrow \boxed{\mathbf{B}} \rightarrow \beta$$

Here, we have only a partial knowledge about **B** and are not sure of how it works exactly—that is what we want to find out.

We can use a computational system **C** to simulate the experiment **B** such that when the inputs a correspond to initial conditions α, the outputs b will correspond to the final conditions β. This type of simulation, however, may not be truly realistic in the sense that the information mechanics involved in **C** could be totally different from that in **B.** An extreme example is that we can always use a data-fitting technique to simulate the relation between α and β. In this case, although **C** can produce the same set of inputs and outputs as **B** does under a specific condition, **C** and **B** are not directly comparable. Thus, the complete knowledge of **C** cannot be used to advance our understanding of how **B** works.

A more realistic simulation requires that a clear map exists between the computational elements in **C** and the constituent parts in **B,** and between the information paths in **C** and the physical interactions in **B.** In other words, we need to make sure that **C** and **B** follow the same information

Color Plates for this article are on pages 112–114.

Address reprint requests to Dr. Zou at the Department of Computer Science, Rice University, P.O. Box 1892, Houston, Texas 77251.

Received 20 July 1994; revised 1 November 1994; accepted 1 December 1994

Journal of Molecular Graphics 13:116–121, 1995

655 Avenue of the Americas, New York, NY 10010

0263-7855/95/$10.00
SSDI 0263-7855(94)00018-N

mechanics. Thus, the computational system **C** can be described by some laws of behavior that are similar in form to the physical laws in **B** and are readily comprehended. When **C** simulates **B,** we can obtain not only correct input and output but also some understanding about how **B** works. And we can expect that **C** simulates **B** not only under one set of conditions but under many possible conditions as well.

Generally speaking, the information mechanics of supermacromolecular systems such as muscle filaments has two distinguishing properties: (1) it is distributed and (2) it is concurrent.

The information mechanics is distributed in the sense that there is no central control process. All protein molecules in the system are equally important. Each molecule must make its own "decisions" about its behavior according to its local environmental conditions and, at the same time, be part of the environment of other molecules.

The information mechanics is concurrent in the sense that the activities of all molecules are simultaneous. The behaviors that appear on scales larger than that of a single molecule should emerge hierarchically as the collective effect of the simultaneous behaviors of individual molecules.

In biochemistry, the behavior of a protein molecule is specified by a set of stable configurations and the transition probabilities between these configurations under different conditions. The biochemistry of a protein molecule can be naturally represented by the computation of a finite automaton.

A finite automaton is a computational machine that consists of a finite set of states and rules. The rules determine the state transition of a finite automaton on the basis of its current state and its input.[3] We can let the states of a finite automaton correspond to the stable configurations of a protein molecule, the inputs correspond to the local environmental conditions, and the rules correspond to the dependence of the transition rate of a protein molecule on its current configuration and local environment.

To preserve the basic features of the information mechanics, the computational counterpart of a supermacromolecular system should contain a large number of finite automata. These finite automata must process in a massively parallel fashion without a central controller and must be locally connected such that every automaton can read in the states of its neighbors as a part of its local environmental condition. In literature, a computational machine that has been constructed in such a manner is sometimes called a cellular automaton.[4,5]

Graphic representation plays an important role in this type of modeling. The geometric shape of protein configurations can be an important part of the information mechanics of a biological system. Visualization of the correspondence between the states of automata and the configurations of protein molecules preserves the information mechanics. In many cases, phenomena that emerge at scales larger than that of individual molecules often appear as forms, shapes, and spatial patterns varying with time. Without graphic representation, we will not be able to identify and observe such phenomena in the simulation.

In this article we introduce this novel formalism of simulation by modeling the regulatory behavior of muscle thin filaments. We emphasize the graphic aspect of the model. The detailed discussion from the point of view of muscle biology has been presented in a separate paper.[1]

COMPUTATIONAL ABSTRACTION OF MUSCLE THIN FILAMENTS

The contraction of muscle results from the interaction of two sets of filaments: the thick filaments, composed mainly of myosin; and the thin filaments, composed mainly of actin, tropomyosin, and troponin.

On the thin filament, actin monomers are arranged in a long helical polymer known as F-actin. Tropomyosin molecules form head-to-tail connections and bind to actin. Troponin molecules are bound to each tropomyosin molecule along F-actin. There exists a stoichiometry of seven actin molecules to one tropomyosin and one troponin.

It is generally accepted that the forces that cause filament motion are generated by cross-bridges (myosin S1) that extend radially from the thick filaments and interact cyclically with the thin filaments while hydrolyzing ATP. The regulation of muscle contraction, which is largely due to the association and dissociation of Ca^{2+} to and from troponin C (TnC), has resulted in several models[6–13] all with the common feature that there is strong cooperative behavior between the various components.[14]

The computational abstraction of the thin filament is achieved by considering each actin or troponin molecule as a finite automaton, namely the actin automaton or troponin automaton, and the tropomyosin molecule as a local connection that passes the state information of an actin or a troponin automaton to its nearby neighbors.

With respect to the binding of myosin S1, an actin monomer on the thin filament has at least two stable configurations. The inactive configuration, denoted by s_1, corresponds to weakly bound S1 or no S1 bound and the active configuration, denoted by s_2, corresponds to the strongly bound S1. The configurational change of an actin monomer corresponds to the association or dissociation of S1 and can be described as

$$s_1 \underset{k_{21}}{\overset{k_{12}}{\rightleftharpoons}} s_2 \qquad (1)$$

where k_{12} and k_{21} are association and dissociation rate constants, respectively. Equation (1) can also be considered as the description of state transitions of an actin automaton. Within a unit of time, the transition probability of an actin automaton from state s_1 to s_2 is $k_{12} \times [S1]$ and from state s_2 to s_1 is k_{21}, where [S1] stands for the concentration of S1. The state transition of an actin automation will be influenced by the states of its neighbors (the neighborhood configuration). The rate constant k_{12} of a given actin automaton depends on the neighborhood configuration of the actin automaton and can be described by a set of local transition rules.[1]

With respect to the binding of Ca^{2+}, each troponin molecule on the thin filament also has at least two stable configurations. The inhibiting configuration denoted by s_3 corresponds to non-Ca^{2+}-bound TnC and the facilitating configuration denoted by s_4 corresponds to Ca^{2+}-bound TnC.

The configurational change of troponin molecule can be described as

$$s_3 \underset{k_{43}}{\overset{k_{34}}{\rightleftharpoons}} s_4 \qquad (2)$$

where k_{34} and k_{43} are the association and dissociation rate constants of Ca^{2+} to and from TnC, respectively. As before, Eq. (2) describes the state transition of a troponin automaton. The transition rate constant k_{34} of a given troponin automaton depends on the neighborhood configuration of the troponin automaton and is also described by a set of local transition rules.

The exact form of the local transition rules, once identified, will provide a quantitative understanding of the cooperativity between the constituent protein molecules on the thin filament, and at the same time allows the automata system to mimic muscle filaments under a wide range of experimental conditions.[1] The transition rate constants in the rules are fundamentally different from simple data-fitting parameters in the following ways: (1) the transition rate constants have clear physical meaning and correspond to well-defined chemical processes; (2) the transition rate constants can be independently measured, in principle, without referring to any specific model; and (3) once the values of the rate constants are determined, either by direct experiment or by comparisons of the model with certain data sets, they are not allowed to have multiple values for comparison with different experimental data.

In the real system, molecules communicate with each other through physical interactions that are largely expressed by tropomyosin molecules. In the corresponding computational system, these physical interactions are represented by local connections (Figure 1).

The computational simulation of the thin filament begins with arrays of finite automata distributed in states s_1, s_2, s_3 and s_4, which represent the initial condition of the thin filament. There is a set of parameters that represents $[Ca^{2+}]$, [S1], [ATP], and so on, and can be read by every finite automaton. At time step 0, all automata start to check the states of their neighbors, then make decisions about their state transitions according to the corresponding local transition rules. After all state transitions are decided, the automata in the system update their states at the same time, which results in a new generation of automata arrays at time 1. By repeating this procedure, we can generate a sequence of automata arrays at discrete time intervals. This sequence, if it contains enough automata, can simulate both the equilibrium and dynamic experimental measurements of the thin filament. Simulations corresponding to various types of experiments were performed that showed excellent agreement with the real data.[1]

GRAPHIC REPRESENTATION

So far we have considered the behavior of the protein molecules from only the functional perspective, in which the configurations of a molecule are defined as biochemically distinguishable species. On the other hand, experiments based on electron microscopy and X-ray diffraction have revealed many structural details about the protein molecules on the thin filament and many hypotheses regarding the structure–function relationship have also been proposed. The correspondence between the state of a finite automaton and the configuration of a protein molecule seems to provide a framework in which the functional and structural information can be combined in a quantitative way by using computer graphics. In this section we discuss the graphic representation for the simulation of the muscle thin filament. Before going to the structural details, we first discuss a useful and simple representation of the simulation.

Abstract representation

The concurrent state transition of a large number of finite automata can be simply visualized by representing the automata array as a one-dimensional lattice. We let each lattice site represent a finite automaton and the color of the lattice site represent the state of the automaton. For example, we can represent an inactive actin by a green lattice site, an active actin by a red lattice site, a facilitating troponin by a yellow lattice site, and an inhibiting troponin by a black lattice site. The simulation process corresponds to the evolution of the lattice. At each time step, a new "generation" of the lattice that shows a new spatial distribution of automata over different states will be produced by the model. We attach the new generation of lattice below the old one so that we can also see the state change of each individual automaton in the time dimension. Thus, this type

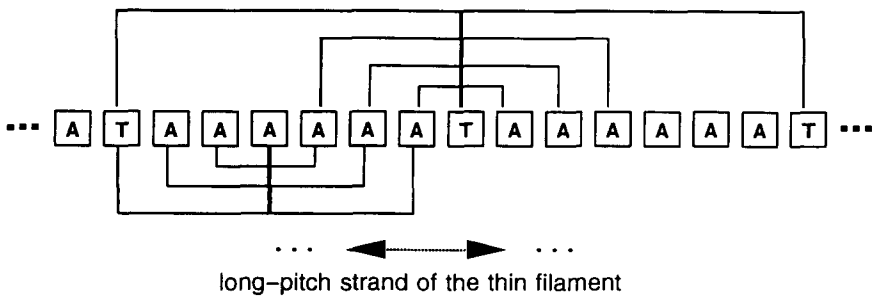

Figure 1. The local connections in the automata array. The actin monomers on a long-pitch strand of the thin filament can be mapped into a one-dimensional array of finite automata. Each actin automaton (labeled A) is connected to its first-, second-, and third-nearest neighbors. At every seventh actin automaton, there is a troponin automaton (labeled T). The behavior of a troponin automaton is influenced by the states of its first-, second-, third-, and seventh-nearest neighbors on the automata array. Note that the seventh nearest neighbors of a troponin automaton are also troponin automata.

of representation enables us to view the binding processes of myosin to actin from both temporal and spatial perspectives at the same time. As an example, Color Plate 1 shows a one-step evolution of a portion of the automata array.

The evolutions of the automata array shown in Color Plate 2 correspond to a dynamic simulation of the thin filament in response to a calcium burst. At time 0, calcium concentration is low (pCa 7.5) and almost all troponin units are in the inhibiting state. Myosin binding is extremely rare at this time. The calcium concentration increases slowly at first. It starts to burst dramatically around step 85 and reaches the maximum at step 125. The transient of calcium concentration was calculated according to the observed aequorin light emission from the experiments of a single frog skeletal muscle fiber.[15] From Color Plate 2, we can see how calcium concentration regulates the association and dissociation of myosin heads to and from the thin filament through the state change of troponin units. The activation is seen to occur in patches, with some parts of the thin filament more active than others. Implications of this stochastic "patchiness" are not clear, but it may be important to consider when discussing overall aspects of force development.

Visual representation

Molecule drawing algorithm In many cases, the three-dimensional structure of a protein molecule contains several distinguishable domains, which may again contain subdomains. The shape, size, and location of these domains and subdomains are determined by the way that the protein molecule is folded. The structure of a protein molecule could be described in terms of domains even when the structural data are only at low resolution. In this study, the three-dimensional shape of a protein molecule is represented by an isosurface of the electron density of the molecular system. Domains are the basic graphic objects involved in the generation of the surface.

For a supermacromolecular system such as the actin filament, suppose that there are N protein molecules bound to each other and that the molecule α contains m_α domains ($\alpha = 1,2, \ldots, N$). The position of molecule α can be described by a three-dimensional vector $\mathbf{p}_\alpha$. The position of the domains in molecule α with respect to $\mathbf{p}_\alpha$ can be described by a set of vectors $\mathbf{d}_{\alpha\beta}$ ($\beta = 1,2, \ldots, m_\alpha$). In a given orthogonal coordinate system with a unit vector set $\{\mathbf{i}, \mathbf{j}, \mathbf{k}\}$, the position vector of domain β in molecule α can be expressed as

$$\mathbf{p}_\alpha + \mathbf{d}_{\alpha\beta} = \mathbf{r}_{\alpha\beta} = x_{\alpha\beta}\mathbf{i} + y_{\alpha\beta}\mathbf{j} + z_{\alpha\beta}\mathbf{k} \qquad (3)$$

We assume that the electron distribution of each domain can be approximated by a three-dimensional Gaussian function and that the electron density function of the whole system equals the summation of the contributions from every individual domain. In other words, the electron density of the supermacromolecular system can be expressed as a function of the space vector $\mathbf{r}$ ($\mathbf{r} = x\mathbf{i} + y\mathbf{j} + z\mathbf{k}$):

$$\rho(\mathbf{r}) = C \sum_{\alpha=1}^{N} \sum_{\beta=1}^{m_\alpha} \exp\left[-\left(\frac{x - x_{\alpha\beta}}{\sigma_x^{\alpha\beta}}\right)^2 - \left(\frac{y - y_{\alpha\beta}}{\sigma_y^{\alpha\beta}}\right)^2 - \left(\frac{z - z_{\alpha\beta}}{\sigma_z^{\alpha\beta}}\right)^2 \right] \qquad (4)$$

where C is a normalization constant and the parameters $\sigma_x^{\alpha\beta}$, $\sigma_y^{\alpha\beta}$, and $\sigma_z^{\alpha\beta}$ are the dimensional measurements of domain β in molecule α along the directions **i**, **j**, and **k**, respectively.

The isosurface of the electron density of the molecular system is drawn according to the following procedure in general: (1) calculate vectors $\mathbf{p}_\alpha$ and $\mathbf{d}_{\alpha\beta}$ on the basis of the current structural understandings of the molecular system; (2) specify parameters $\sigma_x^{\alpha\beta}$, $\sigma_y^{\alpha\beta}$, and $\sigma_z^{\alpha\beta}$ on the basis of the measurements of the domains and the bound connections between them; (3) if possible, calculate the alterations on $\mathbf{p}_\alpha$, $\mathbf{d}_{\alpha\beta}$, $\sigma_x^{\alpha\beta}$, $\sigma_y^{\alpha\beta}$, and $\sigma_z^{\alpha\beta}$ corresponding to the distortion of the shape of domains during the configurational change of each molecule; (4) determine the threshold value of the electron density for an isosurface of Eq. (4); (5) calculate the vertices and the surface normals of the isosurface according to an appropriate algorithm such as the "marching cubes"[16]; (6) draw the isosurface by using vertex subroutines such as those in *SGI Graphics Library*[17]; (7) if possible, compare the calculated image with the three-dimensional reconstruction data of electron microscopy; (8) repeat steps (2) to (7) until a satisfactory representation is reached.

F-actin helix and myosin subfragment 1 The F-actin helix can be regarded as a two-stranded structure with a half-pitch of about 37 nm and a diameter of 9 to 10 nm. Electron microscopy and three-dimensional reconstruction techniques have been used to visualize the geometric shape of real F-actin filaments.[18–20] The bulk of the actin monomer is about 5.5 × 5.5 × 3.5 and is composed of two domains. The "large" inner domain contains subdomains 3 and 4, whereas the "small" outer domain contains subdomains 1 and 2. The long axis of the monomer lies roughly perpendicular to the filament axis.[21] The myosin subfragment 1-binding sites lies on subdomain 1 of actin.[22] The myosin head approaches the actin filament tangentially and binds to a single actin.

The graphic representation of F-actin is constructed on the basis of a reduced atomic model.[20] The electron density of each of the four subdomains in an actin monomer is approximated by a three-dimensional Gaussian function. The parameters $\sigma_x^{\alpha\beta}$, $\sigma_y^{\alpha\beta}$, and $\sigma_z^{\alpha\beta}$ are determined on the basis of the mass of the subdomains and the putative bonds between them. The density function of the F-actin at a given point is then calculated according to Eq. (4). We assume that the contribution to the density function from actin monomers that lie beyond the five nearest ones are negligible. Therefore, in the calculation of Eq. (4), we consider only the 20 subdomains in the 5 nearest actin molecules.

A simplified algorithm is used here to calculate the isosurface. In a cylindrical coordinate system $\{r, \phi, z\}$, we let the z axis of the coordinate system coincide with the helical axis of the F-actin filament. The vertices of the isosurface are determined by searching r values for all ϕ that have positive surface normals. To make an efficient rendering, surface coordinates of F-actin are written into a data file and the distortions of the shape of the actin monomer caused by the binding of the myosin head are ignored.

A similar approach is also used to create the three-dimensional shape of myosin subfragment 1 on the basis of structural data.[22,23] The vertices data of the myosin head is recorded. Myosin heads are placed to the binding sites on actin monomers by applying translations and rotations on

the recorded vertices data. A graphic representation of the binding of myosin S1 to F-actin is shown in Color Plate 3.

Tropomysin filament and troponin unit A tropomyosin molecule is about 41 nm long and is almost a fully α-helical coiled coil.[24] On the basis of X-ray results,[25] together with an analysis of amino acid sequence periodicities, more detailed structural information can be inferred. Tropomyosin molecules form head-to-tail connections and each tropomyosin molecule appears to display a set of discrete binding sites that permits weak linkages of the flexible tropomyosin filament to F-actin along the long-pitch helical strands.[12,26] A three-dimensional reconstruction of thin filament electron micrographs confirms that a movement of tropomyosin on thin filament occurs on the binding of Ca^{2+} to TnC.[27]

In our graphic representation, tropomyosin is approximated by flexible coiled tubes. Each tropomyosin molecule covers seven actin sites (Color Plate 4). The binding of a myosin head to an actin site can change the tropomyosin position locally around the actin site as well as that around the first-, second-, and third-nearest neighboring actin sites (Color Plate 4). The exact position of the tropomyosin at a certain actin site is determined by the configurations of the actin site, the first-, second-, and third-nearest neighbors of the actin site, and the nearest troponin molecule.

Troponin, a Ca^{2+}-sensitive complex, has three subunits: TnC, TnI, and TnT. Troponin T binds one troponin complex to each tropomyosin molecule at intervals of 38 nm along F-actin. The troponin complex has an elongated shape with TnC and TnI forming a globular "head" region and TnT a long "tail."[28] An X-ray structure study[29] indicated that the amino-terminal tail end of TnT spans the head-to-tail joint of tropomyosin filaments, and that the head region of the troponin complex binds about 20 nm away, near residues 150–180 of the tropomyosin molecule. Although many aspects about the structure of troponin and its binding to actin remain ambiguous, a simple graphic representation is proposed (Color Plate 5). As shown in Color Plate 5, there are two stable states for each troponin molecule: one corresponds to Ca^{2+}-bound TnC and the other corresponds to non-Ca^{2+}-bound TnC.

Dynamics of the thin filament Putting the above-described graphic representations together, we can see that the states of the automata array at any given time step can be directly mapped into the geometric shapes of protein configurations (Color Plate 6). A dynamic simulation can thus be viewed in the form of video images. This allows us to investigate various processes on thin filaments not only in temporal and spatial dimensions, but also from the structural perspective. For example, the dynamic simulation of thin filaments shown in Color Plate 2 can be represented as a three-dimensional graphic animation (see http://www-bioc.rice.edu/Bioch/Phillips/Zou/). Color Plate 7 shows a sequence of video images corresponding to the evolution of the automata array from time step 110 to 119 in Color Plate 2. The length of the time step in the simulation is 1 to 10 ms.[1]

The diffusion processes of myosin heads and Ca^{2+} particles in the solution as seen in Color Plate 7 are simulated by a three-dimensional cellular automaton with a set of collision and movement rules. The simulation of the diffusion of myosin head and calcium particles was coupled with the simulation of thin filaments through an interface control and displayed by the animation program.

Implementation

The simulation package is written in C and the interface is developed for X11. The program can run on UNIX machines and, by using data parallel software or by following a message-passing scheme, the program is ready to use parallel processing power of parallel or distributed machines. The abstract graphic representation of the automata array as well as the data collection and display are integrated parts of the simulation program.

The three-dimensional animation is also written in C and uses *SGI Graphics Library*. It is developed as an independent package to the simulator and can be connected to the simulator through socket network communications. The simulation and graphic display can be run in parallel. All geometric shapes are drawn by using vertex-drawing subroutines of *SGI Graphics Library* in RGB mode. Each graphic scene of the animation can be recorded automatically in various formats or can be appended to a video file.

CONCLUSION AND DISCUSSION

In this article we describe a novel formalism for computational simulation by modeling the regulatory behavior of muscle thin filaments as an example. By using computer graphics, we can create a "surrogate reality" in the sense that (1) each finite automaton in our computational system corresponds to a protein molecule on the thin filament; (2) the location of the finite automaton with respect to other finite automata corresponds to the physical location of the protein molecule with respect to other constituent molecules on the thin filament; (3) the state of a finite automaton in the model represented by a geometric shape corresponds to a certain configuration of a protein molecule on the thin filament; (4) the state transition of a finite automaton in the model represented by a change of its geometric shape corresponds to the configurational change of a protein molecule on the filament; (5) the connection of the finite automaton with its neighbors represented by the contact of the geometric shapes and by the local disturbance caused by the changes of shapes corresponds to the physical interactions between the protein molecules on the filament; and (6) the law that we used to describe the computational model, that is, Eqs. (1) and (2), are in the exact same form as that we used to describe the behavior of the thin filament in biochemical experiments.

The model can serve as an efficient knowledge organization scheme in which all type of results can be integrated into a coherent description of the system as a whole. Meanwhile it also provides a powerful tool with which we can explore and test various hypotheses, both quantitatively and visually, about the unknown aspects of muscle.

ACKNOWLEDGMENTS

This work was supported by the W.M. Keck Center for Computational Biology, the National Library of Medicine training grant LM07093, grant C-1142 from the Robert A. Welch Foundation, and NIH grant AR37264.

REFERENCES

1 Zou, G. and Phillips, G.N., Jr. A cellular automaton model for the regulatory behavior of muscle thin filaments. *Biophys. J.* 1994, **67,** 11–28

2 Toffoli, T. Physics and computation. *Int. J. Theor. Phys.* 1982, **21,** 165–174

3 Hopcroft, J.E. and Ullman, J.D. *Introduction to Automata Theory, Languages, and Computation.* Addison-Wesley, Redwood City, CA, 1979

4 Burks, A.W. *Essays on Cellular Automata.* University of Illinois Press, Urbana, IL, 1970

5 Wolfram, S. Cellular automata as models of complexity. *Nature (London)* 1984, **311,** 419

6 Hill, T.L., Eisenberg, E., and Greene, L. Theoretical model for the cooperative equilibrium binding of myosin subfragment 1 to the actin-troponin-tropomyosin complex. *Proc. Natl. Acad. Sci. U.S.A.* 1980, **77,** 3186–3190

7 Hill, T.L. Two elementary models for the regulation of skeletal muscle contraction by calcium. *Biophys. J.* 1983, **44,** 383–396

8 Brandt, P.W., Cox, R.N., Kawai, M., and Robinson, T. Regulation of tension in skinned muscle fibers. *J. Gen. Physiol.* 1982, **79,** 997–1016

9 Brandt, P.W., Cox, R.N., and Kawai, M. Can the binding of Ca^{2+} to two regulatory sites on troponin C determine the steep pCa/tension relationship of skeletal muscle? *Proc. Natl. Acad. Sci. U.S.A.* 1980, **77,** 4717–4720

10 McKillop, D.F.A. and Geeves, M.A. Regulation of the acto-myosin subframent 1 interaction by troponin/tropomyosin. *Biochem. J.* 1991, **279,** 711–718

11 Tobacman, L.S. and Adelstein, R.S. Mechanism of regulation of cardiac actin-myosin subfragment 1 by troponin-tropomyosin. *Biochemistry* 1986, **25,** 798–802

12 Phillips, G.N., Jr., Fillers, J.P., and Cohen, C. Tropomyosin crystal structere and muscle regulation. *J. Mol. Biol.* 1986, **192,** 111–131

13 Williams, D.L., Jr., Greene, L.E., and Eisenberg, E. Cooperative turning on of myosin subframent 1 adenosinetriphosphatase activity by the troponin-tropomyosin-actin complex. *Biochemistry* 1988, **27,** 6987–6993

14 Chalovich, J. Actin mediated regulation of muscle-contraction. *Pharmacol. Ther.* 1992, **55,** 95–148

15 Konishi, M., Wakabayashi, K., Kurihara, S., Higuchi, H., Onodera, N., Umazume, Y., Tanaka, H., Hamanaka, T., and Amemiya, Y. Time-resolved synchrotron X-ray diffraction studies of a single frog skeletal muscle fiber. *Biophys. Chem.* 1991, **39,** 287–297

16 Wyville, G., McPheeters, C., and Wyville, B. Data structures for soft objects. *The Visual Computer.* 1986, **2,** 227–234

17 Silicon Graphics, Inc., Mountain View, California

18 Orlova, A. and Egelman, E.H. A conformational change in the actin subunit can change the flexibility of the actin filament. *J. Mol. Biol.* 1993, **232,** 334–341

19 Orlova, A., Yu, X., and Egelman, E.H. Three-dimensional reconstruction of a co-complex of F-actin with antibody Fab fragments to actin's NH_2 terminus. *Biophys. J.* 1994, **66,** 276–285

20 Holmes, K.C. and Kabsch, W. Muscle proteins: Actin. *Current Opin. Struct. Biol.* 1991, **1,** 270–280

21 Milligan, R.A. and Flicker, P.F. Structural relationships of actin, myosin, and tropomyosin revealed by cryo-electron microscopy. *J. Cell Biol.* 1987, **105,** 29–39

22 Rayment, I., Holden, H.M., Whitaker, M., Yohn, C.B., Lorenz, M., Holmes, K.C., and Milligan, R.A. Structure of the actin-myosin complex and its implications for muscle contraction. *Science* 1993, **261,** 58–65

23 Winkelmann, D.A., Baker, T.S., and Rayment, I. Three-dimensional structure of myosin subfragment-1 from electron microscopy of sectioned crystals. *J. Cell Biol.* 1991, **114,** 701–713

24 Cohen, C. and Szent-Györgyi, A.G. *J. Am. Chem. Soc.* 1957, **79,** 248

25 Whitby, F.G., Kent, H., Stewart, M., Xie, X., Hatch, V., Cohen, C., and Phillips, G.N., Jr. Structure of tropomyosin at 9 angstroms resolution. *J. Mol. Biol.* 1992, **227,** 441–452

26 Hitchcock, S., DeGregori, S.E., and Varnell, T.A. Tropomyosin has discrete actin-binding sites with sevenfold and fourteenfold periodicities. *J. Mol. Biol.* 1990, **214,** 885–896

27 Lehman, W., Craig, R., and Vibert, P. Ca^{2+}-induced tropomyosin movement in *Limulus* thin filaments revealed by three-dimensional reconstruction. *Nature (London)* 1994, **368,** 65–67

28 Flicker, P.F., Phillips, G.N., Jr., and Cohen, C. Troponin and its interactions with tropomyosin. *J. Mol. Biol.* 1982, **162,** 495–501

29 White, S.P., Cohen, C., and Phillips, G.N., Jr. Structure of co-crystals of tropomyosin and troponin. *Nature (London)* 1987, **325,** 826–828